

Purple Membrane Induced Alignment of Biological Macromolecules in the Magnetic Field

Jürgen Sass,[†] Florence Cordier,[†] Astrid Hoffmann,[†] Marco Rogowski,[‡] Anne Cousin,[†] James G. Omichinski,^{†,||} Hartmut Löwen,[§] and Stephan Grzesiek^{*,†,‡}

Contribution from the Institute of Structural Biology, IBI-2, Forschungszentrum Jülich, 52425 Jülich, Germany, Institute of Physical Biology, Heinrich-Heine-Universität, 40225 Düsseldorf, Germany, and Institute of Theoretical Physics, Heinrich-Heine-Universität, 40225 Düsseldorf, Germany

Received November 9, 1998. Revised Manuscript Received January 11, 1999

Abstract: The general possibility to align biological macromolecules in the magnetic field by the presence of orienting agents such as lipid bicelles has led to a wealth of new structural parameters which can be derived from residual tensorial interactions in high resolution NMR. Here, we report that alignment of water soluble biomacromolecules can be achieved in the presence of the naturally occurring two-dimensional crystals (purple membrane) of the membrane protein bacteriorhodopsin. The extent of the alignment is tunable by the concentration of purple membranes and by the addition of salt which reduces the strength of the electric interaction between solute macromolecule and the membrane. At very high salt concentrations the purple membrane suspension undergoes a phase transition to a very viscous state. In this state, rotation of the membranes is hindered such that the orientation of the membrane patches persists even in the absence of a magnetic field. The induced alignment of solute molecules is shown for the two proteins, ubiquitin and p53, with residual dipolar one-bond ¹H–¹⁵N couplings in the order of 20 Hz. A concept for the description of the irreducible components of the alignment tensors as a linear vector space is presented. In the case of ubiquitin, the direction of the alignment tensor differs strongly from the alignment tensor observed in DMPC/DHPC bicelles. This offers the possibility of an accurate triangulation of the bond vector direction from a combination of the two alignment experiments.

Introduction

The weak alignment of biological macromolecules in magnetic fields has led to a wealth of new structural parameters which can be derived from residual tensorial interactions in high-resolution NMR.^{1,2} Such alignment has been achieved by the intrinsic anisotropy of the macromolecular magnetic susceptibility^{3–5} and by the presence of planar lipid bicelles^{6–8} in aqueous solution. The stronger alignment in the latter case results from steric and electric interactions of the dissolved biomacromolecules with the electrically neutral or weakly charged lipid bicelles.^{2,9,10} Very recently, induced alignment of biomacromolecules has also been reported in the presence of strongly aligned rod-shaped viruses and phages.^{11,12}

Purple membranes (PM) are naturally occurring two-dimensional crystals of the membrane protein bacteriorhodopsin. They are disklike particles with a typical diameter of about 0.75 μm¹³ and a thickness of 49 Å.^{14,15} The P3-symmetric PM crystal has a lattice constant of 63 Å and contains one bacteriorhodopsin monomer in its asymmetric unit.^{14,15} This monomer is surrounded by seven to eight mostly negatively charged lipids.¹⁶ Purple membrane is an extraordinary stable biocrystal. The tertiary structure of bacteriorhodopsin and its organization in the purple membrane are preserved for pH values from ~2.5 to ~10, ionic strengths of up to 5 M, and a temperature range from –269 to 69 °C.^{17,18}

The anisotropy of the magnetic susceptibility per bacteriorhodopsin monomer within the purple membrane (including lipids) has been determined as 1.2×10^{-2} J/mol/T₂.¹³ A typical purple membrane sheet of 0.75-μm diameter contains about 4×10^4 such units. Consequently, the energy of the magnetic alignment for a whole purple membrane crystal, $\chi_{PM}B^2/2$, is more than 1 order of magnitude larger than the thermal energy

[†] Institute of Structural Biology.

[‡] Institute of Physical Biology.

[§] Institute of Theoretical Physics.

^{||} Present address: Department of Biochemistry and Molecular Biology, University of Georgia, Athens, GA 30602.

(1) Saue, A.; Englert, G. *Phys. Rev. Lett.* **1963**, *11*, 462–465.

(2) Tjandra, N.; Bax, A. *Science* **1997**, *278*, 1111–1114.

(3) Bothner-By, A. A.; Domaille, P. J.; Gayathri, C. *J. Am. Chem. Soc.* **1981**, *103*, 5602–5603.

(4) Bothner-By, A. A. In *Encyclopedia of Nuclear Magnetic Resonance*; Grant, D. M., Harris, R. K., Eds.; Wiley: London, 1996; Vol. 5, pp 2932–2938.

(5) Tolman, J. R.; Flanagan, J. M.; Kennedy, M. A.; Prestegard, J. H. *Proc. Natl. Acad. Sci. U.S.A.* **1995**, *92*, 9279–9283.

(6) Ram, P.; Prestegard, J. H. *Biochim. Biophys. Acta* **1988**, *940*, 289–294.

(7) Sanders, C. R.; Hare, B. J.; Howard, K. P.; Prestegard, J. H. *Prog. Nucl. Magn. Reson. Spectrosc.* **1994**, *26*, 421–444.

(8) Vold, R. R.; Prosser, P. S. *J. Magn. Reson.* **1996**, *B113*, 267–271.

(9) Bax, A.; Tjandra, N. *J. Biomol. NMR* **1997**, *10*, 289–292.

(10) Ramirez, B. E.; Bax, A. *J. Am. Chem. Soc.* **1998**, *120*, 9106–9107.

(11) Clore, G. M.; Starich, M. R.; Gronenborn, A. M. *J. Am. Chem. Soc.* **1998**, *120*, 10571–10572.

(12) Hansen, M. R.; Rance, M.; Pardi, A. *J. Am. Chem. Soc.* **1998**, *120*, 11210–11211.

(13) Lewis, B. A.; Rosenblatt, C.; Griffin, R. G.; Courtemanche, J.; Herzfeld, J. *Biophys. J.* **1985**, *47*, 143–150.

(14) Henderson, R. *J. Mol. Biol.* **1975**, *93*, 123–138.

(15) Blaurock, A. E. *J. Mol. Biol.* **1975**, *93*, 139–158.

(16) Kates, M.; Kushwaha, S. C.; Sprott, G. D. *Methods Enzymol.* **1982**, *88*, 98–111.

(17) Oesterheld, D.; Stoerkenius, W. *Nature New Biol.* **1971**, *233*, 149–154.

(18) Shen, Y.; Safinya, C. R.; Liang, K. S.; Ruppert, A. F.; Rothschild, K. J. *Nature* **1993**, *366*, 48–49.

at room temperature for typical magnetic fields ($B > 10$ T) in high field NMR spectrometers. At such magnetic fields the alignment is close to 100% with the purple membrane normal pointing in the direction of the magnetic field.^{13,19}

Here, we report that biological macromolecules dispersed in a suspension of aligned purple membranes orient themselves relative to the membrane due to anisotropic electric and steric interactions. The extent of the alignment is tunable by the concentration of purple membranes and by the addition of salt which reduces the strength of the electric interaction between solute macromolecule and purple membrane. The induced alignment of solute molecules is shown for the two proteins, ubiquitin and p53, with residual dipolar one-bond $^1\text{H}-^{15}\text{N}$ couplings on the order of 20 Hz. This alignment is comparable to the DMPC/DHPC bicelle system² albeit at considerably lower concentrations of the orienting agent (0.1–0.2% w/v PM). This apparently strong interaction of the proteins with the membrane also leads to a decrease in transverse relaxation times. However, as the interactions are tunable by salt and by the choice of the PM concentration, the reduction of transverse relaxation time can be controlled. In the case of ubiquitin, the direction of the alignment tensor differs strongly from the alignment tensor observed in DMPC/DHPC bicelles. This offers the possibility of a complete determination of bond vector direction from a combination of the two alignment experiments.

At salt concentrations higher than ~ 70 mM NaCl, the purple membrane suspension undergoes a phase transition to a highly viscous state. In this state, rotation of the membranes is hindered to such an extent that the orientation of the membrane patches persists even in the absence of a magnetic field. The phase transition is caused by the screening of the purple membrane's negative charges at high ionic strengths such that attractive forces can overcome the electrostatic repulsion between membrane patches.

Experimental Section

Purple membrane (PM) was isolated from *Halobacterium salinarium* cells, strain S9 as described.²⁰ DMPC/DHPC bicelle suspensions were produced according to Ottiger and Bax²¹ with a ratio (w/w) of DMPC:DHPC of 3.1:1.

Human ubiquitin was derived from a gene described by Lazar et al.²² This gene was subcloned as a *NdeI*–*EcoRI* DNA fragment into expression vector pET21b⁺. Protein expression from this construct in *Escherichia coli* strain BL21(DE3), uniform enrichment by ^{15}N , and protein purification by ion-exchange and reverse phase chromatography was carried out as described previously for the human Y-Box protein YB1.²³ Uniformly ^{15}N -enriched p53 was prepared as described previously.²⁴

For the NMR experiments, typically 250- μL sample volumes were used in 5-mm Shigemi microcells containing about 0.2–0.8 mM water soluble protein in 95% $\text{H}_2\text{O}/5\%$ D_2O . All NMR data were acquired on a Bruker DMX-600 NMR spectrometer equipped with a triple-axis pulsed field gradient $^1\text{H}/^{15}\text{N}/^{13}\text{C}$ probehead optimized for ^1H detection.

Scalar $^1J_{\text{NH}}$ and dipolar $^1D_{\text{NH}}$ couplings were derived from a doublet-separated sensitivity-enhanced HSQC experiment with ^{15}N -decoupling during data acquisition.^{25,26} The data matrix consisted of $100^* (t_1) \times 512^* (t_2)$ data points (where n^* refers to complex points) with

(19) Neugebauer, D. C.; Blaurock, A. E.; Worcester, D. L. *FEBS Lett.* **1977**, *78*, 31–35.

(20) Bauer, E.; Dencher, N. A.; Heyn, M. P. *Biophys. Struct. Mech.* **1976**, *2*, 79–92.

(21) Ottiger, M.; Bax, A. *J. Biomol. NMR* **1998**, *12*, 361–372.

(22) Lazar, G.; Haendel, T. *Protein Sci.* **1997**, *6*, 1167–1178.

(23) Kloks, C. P. A. M.; Hoffmann, A.; Omichinski, J. G.; Vuister, G. W.; Hilbers, C. W.; Grzesiek, S. *J. Biomol. NMR* **1998**, *12*, 463–464.

(24) Clore, G. M.; Omichinski, J. G.; Sakaguchi, K.; Zambrano, N.; Sakamoto, H.; Appella, E.; Gronenborn, A. M. *Science* **1994**, *265*, 386–391.

acquisition times of 60 ms (t_1) and 53 ms (t_2). Total measuring time was 0.5 h (2.5 h) for ubiquitin (p53). One-dimensional ^{15}N $T_{1\rho}$ measurements were performed by comparing the first increment of a two-dimensional ^{15}N $T_{1\rho}$ experiment²⁷ for various lengths (8, 58, 108, 158 ms) of the ^{15}N spin-lock pulse applied at an RF field strength of 2.8 kHz, carrier position 116.5 ppm. Data sets were processed using the program nmrPipe²⁸ and peak positions determined using the program PIPP.²⁹

Gelation of the PM suspensions by salt was induced inside the magnet as follows. A 5-mm sample tube was prepared containing 433 μL of 13 mg/mL PM suspension in the fluid state (30 mM phosphate, 50 mM NaCl, 95% $\text{H}_2\text{O}/5\%$ D_2O). A droplet of 28 μL of 5 M NaCl solution was then pipetted gently at the meniscus of the PM suspension air/water interface. Immediately afterward, this sample tube was placed into the magnet, avoiding any further turbulence in the liquid, and a persistent quadrupolar splitting of the deuterium resonance of 4 Hz could be observed. After 30 min of “incubation” in the 14 T field at 40 °C, the sample was taken out of the magnet. The sample had undergone a transition to a highly viscous gel-like state, and no movement of liquid was detectable when turning or shaking the sample tube. After the sample was placed back into the spectrometer, the same 4 Hz quadrupolar splitting of the deuterium resonance could be observed.

The linear dichroism of purple membrane suspensions was detected in the absence of the magnetic field by the following method. The beam of a Schott KL1500 lamp was filtered by a Schott OG515/KG1 filter and passed through a linear polarizer. Subsequently the light was passed through the NMR sample tube, and the intensity of the transmitted light was measured by an optical power meter (model 371, Graseby Optronics). Intensity variations were recorded as a function of the angle between the polarizer direction (electric field vector) and the axis of the NMR sample tube. Experiments were carried out at room temperature.

Results and Discussion

Orientation-Induced Shifts and Line Broadening at Low PM Concentrations. As for the DMPC/DHPC bicelle system,⁹ the alignment of the purple membrane in the magnetic field can be established from the residual orientation of water deuterons in the $\text{H}_2\text{O}/\text{D}_2\text{O}$ mixture. This residual orientation of the deuterons results in a detectable quadrupolar splitting of the deuterium resonance. Splittings larger than 2 Hz are easily observable at purple membrane concentrations of more than ~ 7 mg/mL (see below). At lower concentrations of purple membrane, the smaller splitting of the deuterium resonance is not easily detected because of the large deuterium line width. However, at these low concentrations residual orientation of biomacromolecules can still be detected by residual tensorial couplings within the macromolecule. Figure 1 shows small regions of a two-dimensional doublet-separated sensitivity-enhanced $^1\text{H}-^{15}\text{N}$ HSQC for human ubiquitin. The regions are chosen for the ^{15}N upfield and downfield components of the amide $^1\text{H}_{\text{N}}-^{15}\text{N}$ doublet of residues D32 (top) and Q41 (bottom) in human ubiquitin. As compared to the ^{15}N frequency without purple membrane (Figure 1A) a continuous downfield or upfield shift is observed for the two components after the addition of 1.0 (Figure 1B) and 1.9 (Figure 1C) mg/mL PM. The PM-induced shifts are moderate and not localized to certain regions within the molecule. It is therefore very likely that these shifts

(25) Cordier, F.; Dingley, A. J.; Grzesiek, S. *J. Biomol. NMR* **1999**, *13*, 175–180.

(26) Andersson, P.; Annala, A.; Otting, G. *J. Magn. Reson.* **1998**, *133*, 364–367.

(27) Peng, J. W.; Wagner, G. *J. Magn. Reson.* **1992**, *98*, 308–332.

(28) Delaglio, F.; Grzesiek, S.; Vuister, G. W.; Zhu, G.; Pfeifer, J.; Bax, A. *J. Biomol. NMR* **1995**, *6*, 277–293.

(29) Garrett, D. S.; Powers, R.; Gronenborn, A. M.; Clore, G. M. *J. Magn. Reson.* **1991**, *95*, 214–220.

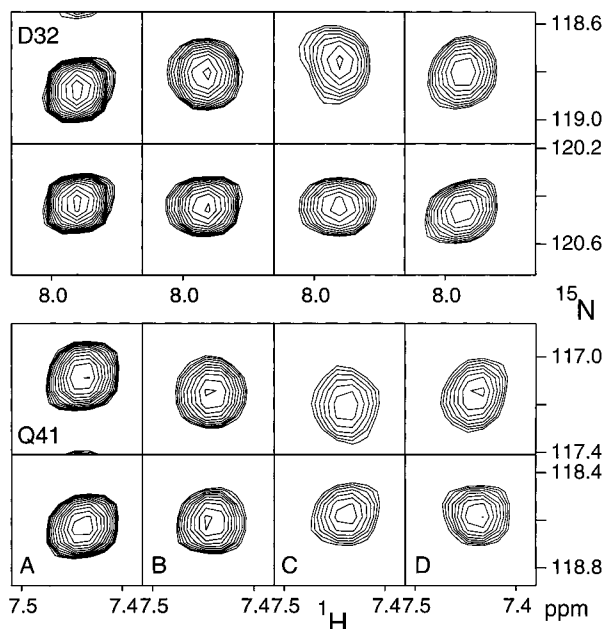


Figure 1. Small regions of a doublet-separated sensitivity-enhanced ^1H - ^{15}N HSQC of ubiquitin for varying concentrations of purple membrane and NaCl. Rows 1–4 show ^{15}N upfield and downfield components of the amides of D32 and Q41. Columns A–D correspond to the following sample conditions: (A) no PM, 0 mM NaCl; (B) 1.0 mg/mL PM, 0 mM NaCl; (C) 1.9 mg/mL PM, 0 mM NaCl; (D) 1.9 mg/mL PM, 50 mM NaCl. Other conditions are described in Table 1.

are due to the residual orientation of ubiquitin and not due to modifications of its structure by the interaction with the PM. Upon addition of 50 mM NaCl (Figure 1D) to the 1.9 mg/mL PM suspension, the PM-induced shift is partially reversed, and the spectral positions and line widths are very similar to the 1.0 mg/mL PM suspension.

The orientation-induced shifts of ^{15}N upfield and downfield components result from the sum and difference of the residual CSA shift and the residual dipolar shift. In general, the shift is more pronounced for the upfield component. The ratio of the induced downfield versus the upfield ^{15}N shift is -0.14 ± 0.36 for the 45 residues of ubiquitin (1.9 mg/mL PM suspension) with an absolute value for the upfield shift larger than 2 Hz. This behavior is a direct consequence of the approximate collinearity of the ^{15}N CSA tensor and the ^1H - ^{15}N dipolar vector.^{30–33} As the line widths in high-resolution NMR are proportional to the square of the local field changes during rotational diffusion, Figure 1 depicts, in a very direct way, the reason for differential line broadening caused by the CSA/dipolar relaxation interference³⁴ in ^1H - ^{15}N amide groups. The larger local field changes for the ^{15}N upfield component lead to stronger transverse relaxation and broader lines.

The addition of purple membrane to the protein solution also leads to a general line broadening and a corresponding intensity loss in the spectra depicted in Figure 1. To quantify this effect, transverse ^{15}N relaxation times were determined from a one-dimensional ^{15}N $T_{1\rho}$ experiment (Figure 2). Compared to

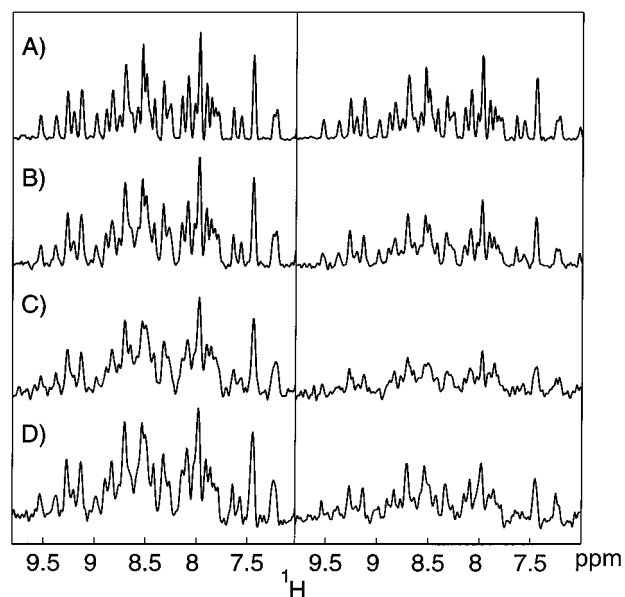


Figure 2. One-dimensional, ^1H -detected ^{15}N $T_{1\rho}$ experiment for ubiquitin at varying concentrations of purple membrane and NaCl. Left side: 8 ms ^{15}N -spin-lock, right side: 58 ms ^{15}N spin-lock. Conditions for rows A–D are identical to the conditions for columns A–D in Figure 1. Spectra have been normalized for equal intensity at 8 ms spinlock duration.

ubiquitin without purple membrane (Figure 2A), the addition of 1.0 (Figure 2B) and 1.9 (Figure 2C) mg/mL purple membrane leads to a continuous decrease in intensity (corresponding to a decrease in ^{15}N $T_{1\rho}$) in the proton-detected spectra for a ^{15}N spin-lock time of 58 ms (Figure 2, right). As for the orientation-induced shift (Figure 1), part of the intensity decrease in the $T_{1\rho}$ experiment is reversed after the addition of 50 mM NaCl (Figure 2D) to the 1.9 mg/mL purple membrane suspension. The intensity ratios in the one-dimensional spectra for ^{15}N spin-lock times of 8 ms (Figure 2, left) and 58 ms (Figure 2, right) correspond to average values for $T_{1\rho}$ of 250 ms (no PM, Figure 2A), 98 ms (1.0 mg/mL PM, Figure 2B), 72 ms (1.9 mg/mL PM, Figure 2C), and 86 ms (1.9 mg/mL PM + 50 mM NaCl, Figure 2D). A very similar reduction is observed for proton transverse relaxation times (T_2) as determined by a 1–1 echo experiment³⁵ (31 ms; 21 ms; 15 ms; 21 ms, for conditions of Figure 2A–D respectively). In contrast, longitudinal ^{15}N relaxation times (T_1) for ubiquitin are virtually unaffected (400–500 ms, not shown) by the addition of purple membrane. A possible explanation for the observed line broadening is anisotropically hindered rotational diffusion in the vicinity of the membrane. This hypothesis is supported by the finding that the ratios of ^{15}N $T_1/T_{1\rho}$ for individual amino acids of ubiquitin in the presence of PM show variations of about 20% within the ordered part of the molecule (J. Sass, unpublished results). These variations in ^{15}N longitudinal and transverse relaxation times are not correlated to similar data observed for the anisotropic diffusion of ubiquitin in the absence of PM.³⁶ Both PM-induced orientation and line broadening are strongly influenced by salt indicating that the interaction between the negatively charged PM and ubiquitin is predominantly electrostatic.

Residual Dipolar Splittings for Ubiquitin. Residual dipolar couplings were determined as the difference of ^{15}N - ^1H splittings observed in the aligned state and in the isotropic state in the absence of an orienting agent. The size of the residual dipolar

(30) Oas, T. G.; Hartzell, C. J.; Dahlquist, F. W.; Drobny, G. P. *J. Am. Chem. Soc.* **1987**, *109*, 5962–5966.

(31) Hiyama, Y.; Niu, C.-H.; Silverton, J. V.; Basovo, A.; Torchia, D. A. *J. Am. Chem. Soc.* **1988**, *110*, 2378–2383.

(32) Shoji, A.; Ozaki, T.; Fujito, T.; Deguchi, K.; Ando, S.; Ando, I. *Macromolecules* **1989**, *22*, 2860–2863.

(33) Lumsden, M. D.; Wasylshen, R. E.; Eichele, K.; Schindler, M.; Penner, G. H.; Power, W. P.; Curtis, R. D. *J. Am. Chem. Soc.* **1994**, *116*, 1403–1413.

(34) Goldman, M. *J. Magn. Reson.* **1984**, *60*, 437–452.

(35) Sklenar, V.; Bax, A. *J. Magn. Reson.* **1987**, *74*, 469–479.

(36) Tjandra, N.; Feller Scott, E.; Pastor Richard, W.; Bax, A. *J. Am. Chem. Soc.* **1995**, *117*, 12562–6.

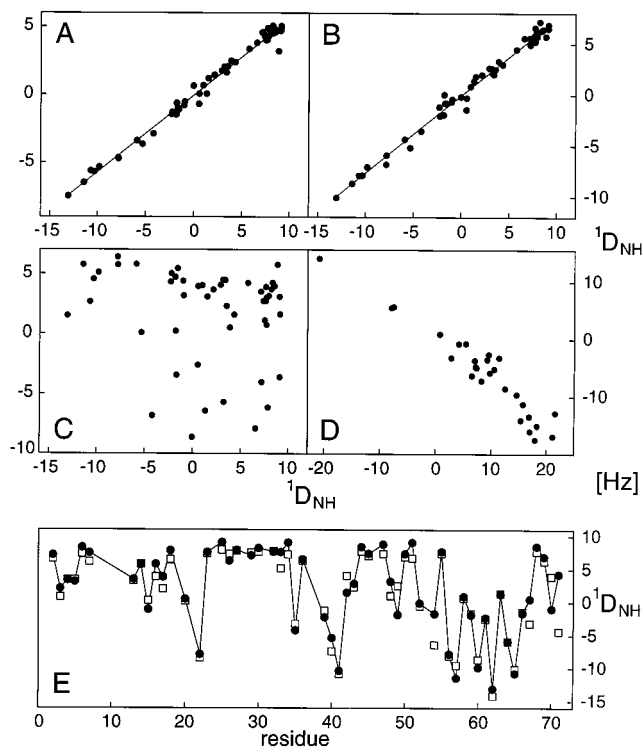


Figure 3. Dipolar couplings ${}^1D_{\text{HN}}$ for ubiquitin and p53 under varying conditions. (A) ubiquitin samples 1 and 2 (see Table 1): 1.0 mg/mL PM (vertical) vs 1.9 mg/mL PM (horizontal). (B) ubiquitin samples 3 and 2: 1.9 mg/mL PM, 50 mM NaCl (vertical) vs 1.9 mg/mL PM, 0 mM NaCl (horizontal). (C) ubiquitin samples 7 and 2: orientation by DMPC/DHPC bicelles (vertical) vs orientation by 1.9 mg/mL PM (horizontal). (D) p53 samples 1 and 2: orientation by DMPC/DHPC bicelles (vertical) vs PM orientation (horizontal). (E) measured (filled circles) and calculated (open squares) dipolar couplings for ubiquitin in the presence of 1.9 mg/mL PM (sample 2) as a function of residue number. HN bond vector orientations were derived from the 1.8-Å X-ray structure.⁴⁶

couplings induced by the 1.9 mg/mL suspension of PM ranges from ~ -13 to 10 Hz. It is comparable to the residual dipolar couplings observed in the presence of about 20–30-fold higher concentrations of DMPC/DHPC bicelles.² A very good linear correlation exists ($r = 0.993$) between the couplings observed at 1.9 and 1.0 mg/mL PM (Figure 3A), indicating that the couplings are approximately proportional to the PM concentration. A similar correlation ($r = 0.994$) is observed between the dipolar couplings at 1.9 mg/mL PM before and after the addition of 50 mM NaCl (Figure 3B).

The orientation experiments with PM can be carried out over the full range of temperatures at which purple membranes (< 70 °C) and the oriented protein are stable in aqueous solution. This is in contrast to the DMPC/DHPC micellar system which allows only temperatures above the lipid phase transition at approximately 25–30 °C.²¹ Residual dipolar couplings for ubiquitin recorded at 15 °C are very similar to the dipolar couplings at 40 °C shown in Figure 3A and B. Quantitative results for these experiments are listed in Tables 1 and 2.

In contrast to these results, no linear correlation exists between the dipolar splittings induced by the PM and the dipolar splittings induced by a 3% (w/v) suspension of DMPC/DHPC bicelles (Figure 3C). The “L-shaped” appearance of this two-dimensional correlation indicates that the molecular orientation tensors for the two alignment systems are not collinear.¹⁰

Orientation Tensors. Conventionally, the three Euler angles and the axial and rhombic components of orientation tensors

have been derived from the measured tensorial interactions and the molecular coordinates by means of a nonlinear least-squares procedure.² Here, we show that this minimization can be reduced to a linear problem by introducing a vector space consisting of the five irreducible components of the Saupe order matrix.³⁷ This concept of a linear vector space also offers a convenient way to quantify the similarity of tensors derived from the different alignment experiments by means of the canonical scalar product. In addition, the irreducible components of the Saupe order matrix relate in a transparent way to the energies responsible for the molecular orientation.

Using irreducible tensor notation, the expected dipolar coupling $D_{i,\text{theo}}$ for a certain dipolar vector r_i in the absence of internal motions of the molecule can be expressed as³⁸

$$\begin{aligned} D_{i,\text{theo}} &= (4\pi/5)^{1/2}\kappa \sum_{m=-2,2} \langle D_{m0}^2(\Omega) \rangle Y_{2m}(\theta_i, \phi_i) \\ &= (4\pi/5)^{1/2}\kappa \sum_{m=-2,2} S_m Y_{2m}(\theta_i, \phi_i) := \\ &\quad \sum_{m=-2,2} A_m Y_{2m}(\theta_i, \phi_i) \quad (1) \end{aligned}$$

where $D_{m0}^2(\Omega)$ are elements of the Wigner rotation matrix for Euler angles $\Omega = (\alpha, \beta, \gamma)$ of the molecule with respect to the laboratory frame, $\langle \rangle$ represents an ensemble average over the orientations of the molecule, κ a constant subsuming the dipolar interaction energy and an overall order parameter, Y_{2m} the spherical harmonics, (θ_i, ϕ_i) are the polar angles of the dipolar vector r_i in the molecular frame, and S_m is an irreducible representation of the Saupe order matrix with $S_m^* = (-1)^m S_{-m}$. The five independent parameters S_m relate to the five independent elements of the traceless, symmetric Saupe order matrix³⁷ $S_{\alpha\beta} = \langle 3 \cos \theta_\alpha \cos \theta_\beta - \delta_{\alpha\beta} \rangle / 2$ ($\alpha, \beta = x, y, z$) by a linear transformation³⁸

$$\begin{aligned} S_{xx} &= \left(\frac{3}{8}\right)^{1/2} (S_2 + S_{-2}) - S_0/2 \\ S_{yy} &= -\left(\frac{3}{8}\right)^{1/2} (S_2 + S_{-2}) - S_0/2 \\ S_{zz} &= S_0 \\ S_{xy} &= S_{yx} = -i\left(\frac{3}{8}\right)^{1/2} (S_2 - S_{-2}) \\ S_{xz} &= S_{zx} = \left(\frac{3}{8}\right)^{1/2} (S_1 - S_{-1}) \\ S_{yz} &= S_{zy} = -i\left(\frac{3}{8}\right)^{1/2} (S_1 + S_{-1}) \end{aligned} \quad (2)$$

Once the constants $A_m = (4\pi/5)^{1/2}\kappa S_m$ are calculated from the measured couplings and the molecular coordinates by a linear least-squares fit, $A_{\alpha\beta} = \kappa S_{\alpha\beta}$ is found by eq 2. The principal axis system and eigenvalues of $A_{\alpha\beta}$ can then be derived by standard methods of linear algebra. Table 1 shows the results of this procedure for all experiments in terms of the constants A_m , A_{zz} , $0 \leq \eta = (S_{xx} - S_{yy})/S_{zz} \leq 1$, and Euler angles of the principal axis system.

A convenient way to express the collinearity of two orientation tensors can be established by defining a scalar product $\langle A^1 | A^2 \rangle$ between their two sets of constants A_m^1 and A_m^2 , for

(37) Saupe, A. Z. *Naturforsch.* **1964**, *19a*, 161–171.

(38) Emsley, J. W. In *Encyclopedia of Nuclear Magnetic Resonance*; Grant, D. M., Harris, R. K., Eds.; Wiley: London, 1996; Vol. 4, pp 2788–2799.

Table 1. Fitted Alignment Tensors for Ubiquitin and p53 Dissolved in Purple Membrane or DMPC/DHPC Bicelle Suspensions

sample	ubiquitin 1 ^a	ubiquitin 2	ubiquitin 3	ubiquitin 4	ubiquitin 5	ubiquitin 6 ^b	ubiquitin 7	p53 1	p53 2
PM [mg/mL]	1.0	1.9	1.9	1.9	7.0	12			3.3
DMPC/DHPC (w/v) [%]							3	5	
NaCl [mM]	0	0	50	50	50	350	0	0	0
T [°C]	40	40	40	15	40	40	40	35	35
A _{2r} ^c	0.73	1.30	0.89	-0.37	-4.36	-1.21	0.55	22.72	-31.63
A _{2i}	-5.17	-9.30	-6.98	-5.95	-18.09	-3.29	2.98	-2.36	0.50
A _{1r}	-4.87	-8.13	-6.57	-6.04	-11.78	-5.25	6.68	0.58	-2.33
A _{1i}	-6.06	-10.51	-8.22	-6.59	-7.69	-1.92	-4.43	-1.10	-0.09
A ₀	-1.39	-1.99	-2.15	-1.37	8.25	-0.54	-8.93	10.86	-1.42
A _{zz} ^d	-8.39	-14.55	-11.35	-9.61	-21.38	-5.82	-9.41	-21.09	24.89
η	0.08	0.11	0.09	0.10	0.13	0.30	0.24	0.35	0.94
α ^e	49.85	50.15	49.66	44.81	37.55	29.22	-38.75	87.06	89.54
β	51.38	52.33	50.91	51.73	67.83	52.06	148.52	88.31	90.19
γ	163.01	160.74	162.31	149.58	20.02	47.52	37.92	176.18	175.57
rmsd ^f	1.09	1.97	1.41	1.27	3.09	0.98	0.83	2.05	2.55
Q-factor ^g	0.29	0.30	0.28	0.30	0.29	0.38	0.20	0.22	0.19
N ^h	56	56	56	52	45	56	56	29	28

^a Sample conditions. Ubiquitin 1–7: 0.2–0.4 mM ubiquitin, 30 mM phosphate, pH 7.6; p53 1–2: 0.6–0.8 mM (monomer) p53, 30 mM phosphate, pH 7.6. ^b Salt frozen sample (see text). ^c A_{mr,i} real and imaginary parts of the irreducible alignment tensor defined in eq 1. Values are given in Hz. ^d A_{zz} zz-component of Cartesian alignment tensor in the principal axis system. The individual dipolar coupling D_{i,theo} for a given NH dipolar vector (θ_i, φ_i) is calculated from A_{zz} and the rhombicity η by D_{i,theo} = A_{zz}[(3 cos² θ_i - 1)/2 + η/2 sin² θ_i cos 2φ_i]. The following relation holds: 5/4πA_{mr}A_m^{*} = A_{zz}²(1 + η²/3). Values are given in Hz. ^e Euler angles of the principal axis system. ^f Root mean square deviation of theoretical and calculated dipolar couplings. ^g Quality factor Q defined as rmsd/D_{rms}, where D_{rms} is the root mean square of the measured dipolar couplings. ^h Number of residues used in the fit. Only residues with low internal mobility were considered.

Table 2. Normalized Scalar Products ⟨A¹|A²⟩/⟨A¹|A¹⟩^{1/2}⟨A²|A²⟩^{1/2} between the Fitted Alignment Tensors for Different Ubiquitin Samples in the Presence of Purple Membranes or DMPC/DHPC Bicelles

sample ^a	2	3	4	5	6	7
1	0.9995	0.9999	0.9922	0.8329	0.8629	-0.1445
2		0.9990	0.9909	0.8427	0.8565	-0.1491
3			0.9926	0.8290	0.8636	-0.1345
4				0.8690	0.9086	-0.2006
5					0.8759	-0.5386
6						-0.4916

^a Sample numbering refers to Table 1.

which it is easily shown that

$$\begin{aligned} \langle A^1 | A^2 \rangle &= \sum_{m=-2,2} A^1_m A^{2*}_m = (4\pi/5)\kappa^2 \sum_{m=-2,2} S^1_m S^{2*}_m \\ &= {}^2/{}_3(4\pi/5)\kappa^2 \sum_{\alpha,\beta=x,y,z} S^1_{\alpha\beta} S^2_{\alpha\beta} \end{aligned} \quad (3)$$

The normalized scalar product defined as ⟨A¹|A²⟩/⟨A¹|A¹⟩^{1/2}⟨A²|A²⟩^{1/2} can be identified with the cosine of the angle between the two five-dimensional vectors A¹_m and A²_m. A value of 1 for this normalized scalar product means that the two orientation tensors are collinear, whereas a value of 0 indicates that the two orientation tensors are perpendicular to each other.

The orientation tensors for ubiquitin at purple membrane concentrations below 2 mg/mL are to a very high degree collinear (Table 2). The values for the normalized scalar products between the vectors of their irreducible representations range between 0.9909 and 0.9999 for the experiments carried out at temperatures of 15 °C or 40 °C, PM concentrations of 1.0 or 1.9 mg/mL, and in the absence or presence of 50 mM NaCl. In contrast, these orientation tensors are very different from the orientation tensor derived for ubiquitin aligned by DMPC/DHPC bicelles. The normalized scalar product between the alignment tensor for the lipid bicelles and the PM-aligned state (1.9 mg/mL PM) has a value of -0.15. This indicates almost complete linear independence and an “angle” of cos⁻¹(-0.15) = 99° between the two alignment tensors. The effects of this linear independence are different rhombicities η

(0.11 vs 0.24, Table 1) and a different orientation of the principal axes systems for the two alignment tensors, e.g., the direction of the two z-axes differs by 59°.

Such large differences in orientation are the result of the two different interactions of the protein molecules with the orienting membrane systems. In the DMPC/DHPC bicellar system, presumably steric interactions with the membrane lead to the residual orientation.² In the diluted PM system, the orientation is caused mainly by electrical interactions. In this system, the same degree of orientation can be achieved at about 20–30-fold lower membrane concentrations than in the DMPC/DHPC system. This indicates that the characteristic length of the interaction with the membrane must be larger in the PM system. For electric interactions in solution, an estimate for the characteristic length can be given as the Debye length. The concentrations of phosphate buffer, counterions for ubiquitin and purple membrane, and NaCl correspond to the ionic strength of a monovalent salt solution of ~50–100 mM. For such ionic strengths the Debye length ranges between 10 and 15 Å at the temperatures used in the experiments. Assuming complete orientation of a molecule within a distance of 10 Å to the purple membrane, no orientation outside of this distance, a membrane thickness of 49 Å, and a concentration of 0.2% (w/v ≈ v/v) purple membrane, the residual orientation should be on the order of 0.2% × 2 × 10 Å/49 Å = 8 × 10⁻⁴. This order of magnitude estimate is in good agreement with the degree of orientation corresponding to maximal ¹H–¹⁵N residual dipolar couplings of ~20 Hz.²

Linear Correlations between Different Orientation Tensors. If the above hypothesis is correct, then it should be possible to gradually shift from the alignment by the electric field of the purple membrane to a steric alignment by decreasing the Debye length and increasing the purple membrane concentration. Table 1 lists the ubiquitin alignment tensor for an experiment at higher purple membrane concentration (7 mg/mL) and 50 mM NaCl. The normalized scalar product of this alignment tensor with the alignment tensor at 1.9 mg/mL PM without NaCl is 0.84 (Table 2). On the other hand, the normalized scalar product between the alignment tensors for the high purple membrane concentration and the DMPC/DHPC experiment is

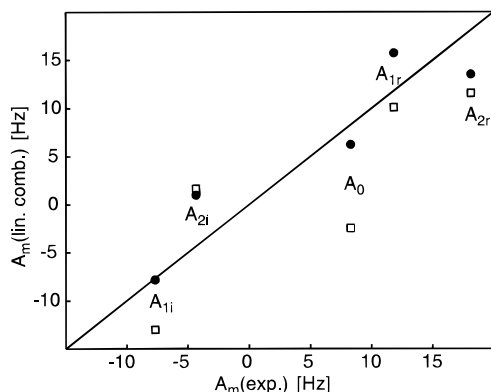


Figure 4. Real and imaginary components of the irreducible representation of the orientation tensor of ubiquitin in the presence of 7.0 mg/mL PM, 50 mM NaCl [$A_m(\text{exp.})$, sample 5, Table 1] vs a best fit (filled circles) linear combination $A_m(\text{linear combination})$ of the orientation tensors at 1.9 mg/mL PM, no NaCl and at 3% (w/v) DMPC/DHPC. $A_m(\text{linear combination}) = 1.15A_m(\text{sample 2}) - 0.95A_m(\text{sample 7})$. Open rectangles depict the case when $A_m(\text{expt})$ is approximated by $A_m(\text{sample 2})$ alone [$A_m(\text{linear combination}) = 1.24A_m(\text{sample 2})$].

-0.54 . Since the corresponding value for the lower PM concentration is only -0.15 , this indicates a stronger collinearity between the tensor for the high PM concentration and the lipid bicelles.

At present, the relation between experimentally determined alignment tensors and specific molecular properties is not completely understood. In the following we show that the alignment tensor for the higher purple membrane concentration can be approximated by a linear combination of the alignment tensor at lower purple membrane concentration (electric orientation) and the alignment tensor for the DMPC/DHPC bicelles (steric orientation). For this decomposition, a fit was carried out which minimizes the square deviation χ^2 between the ubiquitin alignment tensor at high PM concentration (Table 1, sample 5) and a linear combination of the tensor at low PM concentration (sample 2) and the DMPC/DHPC tensor (sample 7)

$$\chi^2 = \|\mathbf{A}(\text{sample 5}) - a\mathbf{A}(\text{sample 2}) - b\mathbf{A}(\text{sample 7})\|^2 \rightarrow \min \quad (4)$$

where $\mathbf{A} = (A_2, A_1, \dots, A_{-2})$ and $\|\mathbf{A}\|^2$ has its standard definition as $\sum_{m=-2,2} A_m A_m^*$. The minimization is linear for the two coefficients a and b . A strong correlation ($r = 0.95$) between all components of the measured alignment tensor and the approximated alignment tensor is observed (Figure 4, filled circles for optimal values of $a = 1.15$ and $b = -0.95$). The root square deviation χ between experimentally determined tensor $\mathbf{A}(\text{sample 5})$ and the fitted tensor $a\mathbf{A}(\text{sample 2}) + b\mathbf{A}(\text{sample 7})$ is 11.5 Hz. This is significantly lower than the deviation that is observed when $\mathbf{A}(\text{sample 5})$ is approximated by a linear least-squares fit to the vector $\mathbf{A}(\text{sample 2})$ alone ($\chi = 18.3$ Hz, Figure 4, open squares).

Recently, a modulation of the alignment tensor of ubiquitin in the DMPC/DHPC system was reported by the successive introduction of positive charges (cetyltrimethylammonium bromide, CTAB) into the lipid bicelles.¹⁰ As shown in the Supporting Information, the alignment tensor for the higher CTAB:lipid ratio can also be approximated by a linear combination of the alignment tensors for the uncharged system and the alignment tensor for the lower CTAB:lipid ratio.

The theoretical justification for such a linear decomposition of the alignment tensors for different alignment systems comes

from the following argument. It is assumed that the probability density $p(\mathbf{\Omega})$ of the Euler angles $\mathbf{\Omega}$ for the orientation of a molecule in solution follows Boltzmann statistics:

$$p(\mathbf{\Omega}) = \int p(\mathbf{\Omega}, \mathbf{r}) d\mathbf{r} = \int \exp(-E(\mathbf{\Omega}, \mathbf{r})/kT) d\mathbf{r} / \int \exp(-E(\mathbf{\Omega}, \mathbf{r})/kT) d\mathbf{r} d\mathbf{\Omega} \quad (5)$$

where $p(\mathbf{\Omega}, \mathbf{r}) d\mathbf{r} d\mathbf{\Omega}$ is the probability of finding the molecule at position \mathbf{r} and Euler angles $\mathbf{\Omega}$, $E(\mathbf{\Omega}, \mathbf{r})$ is the energy corresponding to this position and orientation, and kT is the thermal energy. In general $E(\mathbf{\Omega}, \mathbf{r})$ will contain contributions from all interactions between the molecule and the membrane as well as from exterior anisotropic interactions such as the molecular magnetic susceptibility. If energies $E(\mathbf{\Omega}, \mathbf{r})$ are small compared to kT , the exponential function can be linearized

$$p(\mathbf{\Omega}) \approx \int [1 - E(\mathbf{\Omega}, \mathbf{r})/kT] d\mathbf{r} / N \quad (6)$$

where N is a normalization constant such that $\int p(\mathbf{\Omega}) d\mathbf{\Omega} = 1$. Note that the condition $E(\mathbf{\Omega}, \mathbf{r}) \ll kT$ might not be valid in the proximity of the orienting membrane. For the argument below, however, only the anisotropic parts of the interactions are important. These anisotropic parts are usually smaller than the total energy $E(\mathbf{\Omega}, \mathbf{r})$. Assuming that eq 6 is fulfilled, it is immediately evident that the probability distribution $p(\mathbf{\Omega})$ is a linear function of the different interaction energies leading to the orientation of the molecule. Combining eq 1 and 6 yields

$$A_m (4\pi/5)^{-1/2} / \kappa = S_m = \langle D_{m0}^2(\mathbf{\Omega}) \rangle = \int p(\mathbf{\Omega}) D_{m0}^2(\mathbf{\Omega}) d\mathbf{\Omega} \approx -1/(NkT) \int E(\mathbf{\Omega}, \mathbf{r}) D_{m0}^2(\mathbf{\Omega}) d\mathbf{\Omega} d\mathbf{r} \quad (7)$$

Therefore, under the approximation of eq 6, the orientation tensor should be a linear function of the energy responsible for the orientation. If the interaction energy separates into different independent parts, then the orientation tensors should decompose into linear subparts as well. The observation that the orientation tensor at the higher PM concentration can be expressed as a linear combination of the orientation tensor at low purple membrane concentration and the orientation tensor for DMPC/DHPC is consistent with the concept that the orientational energy for the high PM concentration is a sum of the electrostatic interactions (low PM concentration) and steric interactions (DMPC/DHPC system).

Residual Dipolar Splittings for p53. To apply the orientation by purple membranes to other systems, it proved practical to titrate the protein solution with small amounts of purple membrane suspension. This titration is carried out until there is an appreciable but not too strong effect on the amide proton T_2 of the protein as determined by a 1-1 echo sequence.³⁵ For the protein p53 at pH 7.6, considerable orientation is achieved in the presence of 3.3 mg/mL PM with a reduction of amide proton T_2 's from 19 to 14 ms (35 °C). Figure 3D depicts the measured dipolar couplings for p53 in the presence of purple membrane vs the couplings measured in a 5% DMPC/DHPC (3.1:1) suspension. Again the size of the dipolar couplings is very similar, ranging from ~ -20 to 20 Hz. In this case, a negative, almost linear correlation is observed for the two cases of orientation. Such a correlation is not surprising since the p53 molecule is a tetramer with three perpendicular two-fold axes both in crystalline form³⁹ and in solution.^{24,40,41} It is expected, that the orientation tensors for both methods of orientation

(39) Jeffrey, P. D.; Gorina, S.; Pavletich, N. P. *Science* **1995**, *267*, 1498-1501.

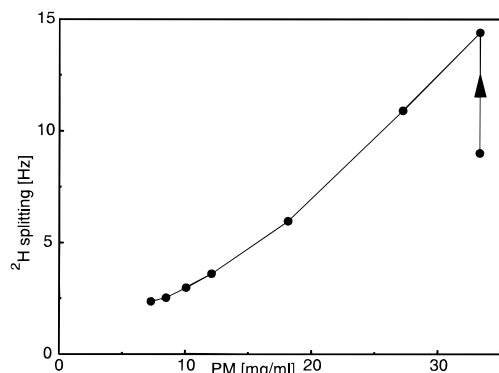


Figure 5. Orientation-induced quadrupolar splitting of the H₂O/D₂O deuterium resonance as a function of purple membrane concentration (30 mM phosphate, pH 7.6, 40 °C). The arrow indicates that the PM suspension was sonicated in a water bath sonifier for 5 min between the recording of the two data points.

should reflect this molecular symmetry. A quantitative analysis of the orientation tensors (Table 1) derived from the dipolar splittings and an X-ray structure (PDB entry 1AIE, 1.5 Å resolution) corroborates this hypothesis. The normalized scalar product between the DMPC/DHPC and PM orientation tensors has a value of -0.95 indicating an almost antiparallel orientation of the two alignment tensors. Within experimental error, the principal axes coordinate system for the two orientation tensors are identical and coincide with the *P422* symmetry axes of the X-ray structure. The three Euler angles for the two orientation tensors agree within $\sim 2^\circ$, corresponding to angles between the corresponding principal axes of the two tensors of less than 3.2° . In addition, the angles between these principal axes and the corresponding symmetry axes of the X-ray structure are smaller than 5° . As the molecular symmetry dictates the orientation of the principal axes of the alignment tensors within the molecule, the different nature of the two orientation mechanisms (steric and electric) can only change the absolute size and rhombicity η of the alignment tensors. In fact, a large difference in rhombicity 0.94 (PM) vs 0.35 (DMPC/DHPC) is observed (Table 1).

Both for ubiquitin and p53, a strong agreement is found between observed dipolar couplings and theoretical dipolar couplings calculated according to eq 1. Figure 2E depicts the calculated and observed couplings for ubiquitin in the presence of 1.9 mg/mL purple membrane. A quantitative measure for the agreement between structure and observed residual dipolar couplings was proposed as the quality factor Q ,⁴² where Q is the ratio of the rmsd between observed and calculated couplings and the rms of the observed couplings (see Table 1). Q -factors calculated in this manner range from 0.19 to 0.38 and are comparable to values given by Cornilescu et al.⁴² for structures and residual couplings of similar quality.

The stability of both ubiquitin and p53 dissolved in the low concentration purple membrane suspension proved to be very high. Over the period of one month, no changes were observed in the NMR spectra of both proteins.

Higher PM Concentrations. At higher PM concentrations (> 7 mg/mL), an orientation-induced residual quadrupolar splitting is easily detectable on the deuterium resonance of the

H₂O/D₂O solvent mixture (Figure 5). In the case of mixed DMPC/DHPC bicelles²¹ such a splitting was attributed to the residual alignment of water molecules rather than to the orientation of deuterons which are in chemical exchange with protonation sites at the membrane water interface. In contrast to the DMPC/DHPC bicelle system, purple membranes contain a high number of hydroxyl groups and other solvent accessible protonation sites which are located both in the lipid headgroups and at the bacteriorhodopsin/water interface. Therefore, chemical exchange of water deuterons as a mechanism for residual orientation cannot be excluded.

Figure 5 shows the orientation-induced splitting of the 95% H₂O/5% D₂O deuterium resonance as a function of purple membrane concentration. A titration by successive dilution was carried out starting at a purple membrane concentration of 33 mg/mL (10 mM phosphate, 25 mM NaCl, pH 7.6). Under these conditions, the membrane suspension is still fluid. The mean distance between individual membrane sheets, however, is considerably smaller than their typical diameter of 0.75 μm . This distance can be estimated as 0.11 μm , assuming dense parallel packing of individual membranes of 49 Å thickness, a unit cell area of the PM P3 lattice of $(63 \text{ \AA})^2 \sin(60^\circ)$ (bacteriorhodopsin trimer), and a molecular weight of 27 kDa for the bacteriorhodopsin monomer. Therefore, at such concentrations, the free rotation and the magnetic alignment of individual membrane sheets are strongly hindered. It was observed that sonication of such a highly concentrated suspension outside of the magnetic field can lead to an increase in the deuterium splitting by more than 50% (Figure 5). Sonication probably removes local stress and induces partial parallel ordering over short ranges. Such partially ordered regions are expected to align themselves more easily in the magnetic field. A subsequent dilution of the suspension with the same buffer solution leads to a gradual decrease of the orientation-induced deuterium splitting. However, the decrease is not completely linear, as its slope becomes smaller at lower concentrations. Apparently, the weaker sterical hindrance at the lower concentrations leads to a better magnetic alignment of individual membrane patches. This compensates in part for the reduction of deuteron alignment resulting from the dilution of the orienting agent. At very low concentrations, where the mean distance between individual membrane patches is larger than the membrane diameter, the orientation-induced quadrupolar splitting is expected to be strictly proportional to the membrane concentration, albeit too small to be observable. Assuming a membrane diameter of 0.75 μm , this condition is fulfilled for PM concentrations smaller than 5 mg/mL.

Gelation of the Purple Membrane Suspension Induced by Salt. During the experiments on the influence of the ionic strength on the orientation of ubiquitin, a phase transition of the purple membrane suspensions from a liquid state to a very viscous state was observed. This state is characterized by a gel-like consistency of the suspension with no macroscopic fluidity detectable by eye. In the absence of divalent cations, the transition to this state occurs after increasing the monovalent salt concentration (NaCl or KCl) above 70–100 mM at pH 7.6. For MgCl₂ the transition is already observed for salt concentrations on the order of 1–5 mM. If the phase transition is induced in the isotropic state of the membrane suspension in the absence of the magnetic field, no dipolar splitting of ubiquitin resonances and no deuterium quadrupolar splitting can be observed after bringing the sample tube into the 14 T magnetic field. Apparently, the viscosity in this state is so high that the frictional

(40) Lee, W.; Harvey, T. S.; Yin, Y.; Yau, P.; Litchfield, D.; Arrowsmith, C. *Nat. Struct. Biol.* **1994**, *1*, 877–890.

(41) Clore, G. M.; Ernst, J.; Clubb, R.; Omichinski, J. G.; Poindexter Kennedy, W. M.; Sakaguchi, K.; Appella, E.; Gronenborn, A. M. *Nat. Struct. Biol.* **1995**, *2*, 321–333.

(42) Cornilescu, G.; Marquardt, J. L.; Ottiger, M.; Bax, A. *J. Am. Chem. Soc.* **1998**, *120*, 6836–6837.

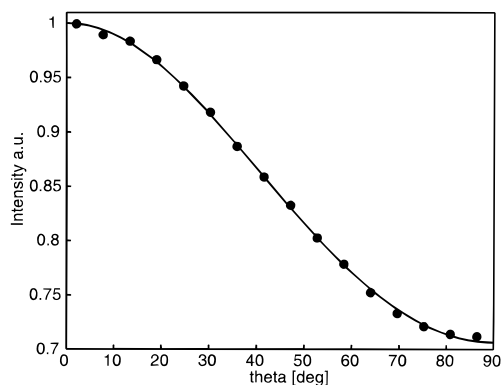


Figure 6. Intensity of polarized light (520–800 nm) passed through the magnetically aligned salt frozen purple membrane suspension in the NMR sample tube as a function of the light polarization direction. Measurements were carried out in the absence of a magnetic field. Θ is defined as the angle between the polarization vector and the axis of the sample tube. The continuous line depicts the result of a best fit to the data according to the function $I_0 \exp(-\epsilon \sin^2 \Theta)$, with $\epsilon = 0.347$, $I_0 = 1$.

forces cannot be overcome by the magnetic torque exerted on the membrane patches.

In contrast, if this salt-dependent gelation is induced inside the magnet in the aligned state of a 13 mg/mL PM suspension (see Experimental Section), then a persistent deuterium quadrupolar splitting of about 4 Hz is observed. The quadrupolar splitting also remains unchanged after repeatedly removing the sample and bringing it back into the magnet. Apparently the purple membrane patches are frozen in the aligned state, and the viscosity of suspension is so high that reorientation to the isotropic state is not possible in the absence of the magnetic field.

Evidence for the persistent alignment in the absence of the magnetic field comes from the strong linear dichroism of such “salt-frozen” purple membrane samples, which is due to the nonisotropic absorbance of the bacteriorhodopsin chromophore retinal.⁴³ Figure 6 depicts the intensity of polarized light (520–800 nm) passed through the sample tube outside of the magnet as a function of the angle Θ between the polarization vector and the axis of the sample tube (direction of the magnetic field and direction of oriented membrane normals). When the electric field vector is parallel to this axis, maximal light intensity is transmitted, whereas a minimum occurs at a 90° angle. This behavior is expected since the absorbance of the chromophores is averaged according to the cylindrical symmetry around the membrane normal and the transition dipole moment of an individual retinal makes a 70° degree angle with respect to this symmetry axis.⁴³ Therefore, the maximal absorption occurs when the electric field vector lies within the membrane plane. The dependence of measured light intensity on the polarization angle Θ is in excellent agreement (Figure 6, solid line) with a theoretical description of the type $I_0 \exp(-\epsilon \sin^2 \Theta)$ where I_0 is the light intensity for $\Theta = 0$ and ϵ is proportional to the difference in the extinction coefficients for light polarized perpendicular and parallel to the membrane normal. This difference in the extinction between the two polarization directions is large enough that the linear dichroism is easily detectable by eye.

The orientation of the PM patches within the gelled sample remains essentially unchanged over the period of several weeks as judged either by the linear dichroism or the residual

orientation of water deuterons detected by the quadrupolar splitting. Apparently, the macroscopic viscosity of the salt frozen PM sample is very high. Nevertheless, it is still possible to introduce other macromolecules into this suspension. For this, the 400 μL “frozen” PM sample was topped with 50 μL of a 2 mM ubiquitin solution. Although the diffusion of the ubiquitin into the gelled sample was hindered, it was complete after ~ 10 days, as judged by the intensity of the ubiquitin NMR signals. The line width of these spectra indicates that the rotational correlation time of ubiquitin molecules within the salt frozen PM suspension is not longer than in the case of lower PM and salt concentrations (data not shown). An analysis of residual dipolar couplings for this sample showed a very similar alignment tensor as for the fluid sample at 7 mg/mL PM, 50 mM NaCl (Tables 1 and 2). These results indicate that high salt concentrations do not preclude the residual orientation of other biomacromolecules, provided that the practical problem to introduce such molecules into the oriented and gelled PM system is overcome.

The principal physical mechanism underlying the salt-induced gelation is the screening of the repulsive electrostatic forces between the negatively charged membrane patches. At high salt concentrations, the screening is so large that attractive forces such as van der Waals or hydrophobic interactions overcome the electrostatic repulsion. As a result, condensation of purple membranes takes place. The phenomenon is very similar to the coagulation of smectic clay suspensions which has been described by statistical models.⁴⁴ It should be noted that this type of coagulation is expected predominantly between the edges of the membrane sheets where the electrostatic repulsion is the weakest. A simplistic description of the purple membrane suspension as a system of charged platelets undergoing mutual van der Waals attraction correctly predicts the observed critical ionic strength for the gelation within an order of magnitude (H. Löwen, unpublished results). Recently, a very similar mechanism has been proposed for the aggregation of charged lipid bicelle systems.⁴⁵

Conclusion

In summary, we have characterized purple membrane suspensions as a system capable of inducing residual orientation of biological macromolecules in the magnetic field. This orientation is on the order of 10^{-3} and comparable to the DMPC/DHPC system. The purple membrane system is extraordinarily stable with respect to a large number of physicochemical parameters. Suspension of purple membranes containing dissolved biomacromolecules are stable on the order of months. In contrast to the steric interaction with DMPC/DHPC, the anisotropic interaction between macromolecules and purple membranes is mainly electrostatic in nature. Since this interaction is stronger than the orienting interaction with the uncharged lipid bicelle system, the same magnitude of orientation is achieved at much lower concentrations of purple membrane. Due to the interaction with the negative membrane, a concomitant decrease in transverse relaxation times is observed which clearly limits the method to molecules where this line broadening is not too strong. However, due to the mechanical stability of the membrane, it is possible to slowly titrate the protein solution with minute amounts of purple membrane such that the line

(44) Dijkstra, M.; Hansen, J.-P.; Madden, P. A. *Phys. Rev. E* **1997**, *55*, 3044–3053.

(45) Losonczi, J. A.; Prestegard, J. H. *J. Biomol. NMR* **1998**, *12*, 447–451.

(46) Vijay-Kumar, S.; Bugg, C. E.; Cook, W. J. *J. Mol. Biol.* **1987**, *194*, 631–544.

(43) Heyn, M. P.; Cherry, R. J.; Müller, U. *J. Mol. Biol.* **1977**, *117*, 607–620.

broadening and the orientation effect can be monitored exactly. In the case of p53 (MWT 20 kDa) a reduction of proton T_2 's by about 27% could easily be afforded given the high sensitivity of experiments for the determination of heteronuclear residual dipolar couplings. Suitable molecules for the PM system are most likely proteins at pH values above their pI and the negatively charged nucleic acids.

Compared to the uncharged lipid bicelle system, the different nature of the orienting interaction for PM also leads to different directions of the orientation tensor within the molecular frame. A simple geometric measure of this difference in orientations is introduced by the scalar product between the irreducible representations of the orientation tensors. The geometric interpretation of the components of the alignment tensor as a linear vector space also leads to a physical picture of the tensor as a linear combination of alignments resulting from different interactions. The validity of this linear approach can be verified for the case of the alignment at higher PM concentrations and for the modulation of DMPC/DHPC alignment tensor by positive charges. For ubiquitin, the scalar product between the DMPC/DHPC and the PM orientation tensors indicates almost

complete linear independence. It is therefore possible to achieve maximal complementary information on the orientation of dipolar vectors from the two orienting systems. The possibility of viewing the dipolar vector and other tensorial interactions from highly different angles represents an initial step toward a complete triangulation of biological macromolecules in solution.

Acknowledgment. We thank Tracy Handel for the gift of the ubiquitin clone as well as Norbert Dencher, Georg Büldt, Stephan Moltke, Andrew Dingley, and Dennis Torchia for valuable discussions. F.C. acknowledges funding by the A. v. Humboldt foundation. This work was supported by DFG grant GR1683/1-1.

Supporting Information Available: Calculation of the linear combinations for the ubiquitin alignment tensors in the DMPC/DHPC/CTAB bicelle system (PDF). This material is available free of charge via the Internet at <http://pubs.acs.org>.

JA983887W